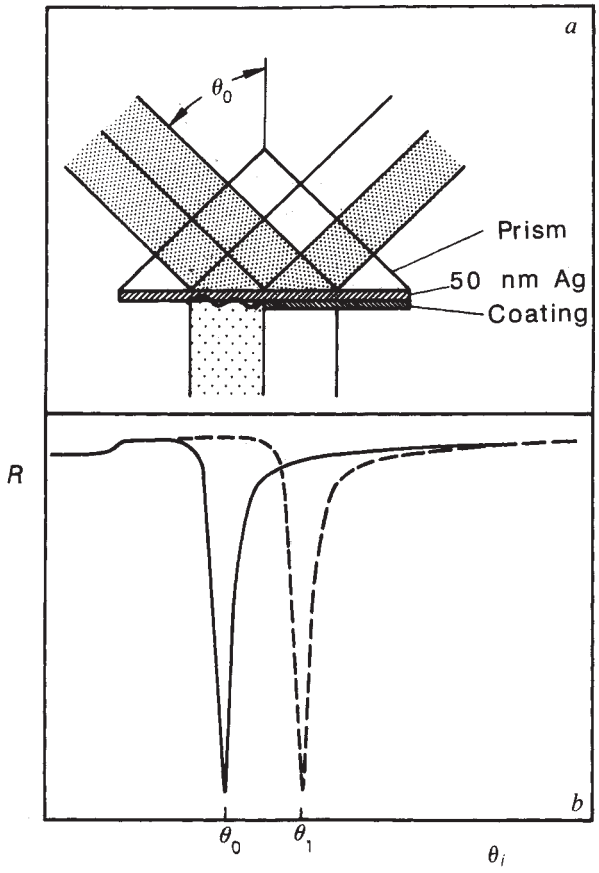

Fig. 4 *a*, Schematic illustration of the contrast mechanism in SPM. Half the silver film is covered by a thin coating which shifts the resonance condition for plasmon coupling. At θ_0 only in the bare silver areas PSP (wavy arrow) are excited. A small fraction of this light is coupled out to the air side, while almost nothing is reradiated to the prism side. The coated regions are off resonance so that all laser light is totally reflected. *b*, Reflectivity, R versus angle of incidence, θ_i, for bare silver (full line) and for coated regions (dashed line).

tivity curve and measured values for the resonance-shift by LB layer coatings.

We suggest that this high sensitivity is because we are dealing with a resonance contrast whereas all other microscope techniques capable of resolving thickness variations in the 10-nm range are, in one way or another, based on interference contrast. Interference curves are, however, much smoother functions than resonance curves.

As for any microscopy, contrast problems in SPM can not be discussed without addressing the question of lateral resolution. Because the detection scheme contains plane-wave optical components, SPM is also limited by diffraction—lateral resolution is in the 1-μm range. If PSP waves are used for the illumination of the object under investigation, additional effects that could reduce the lateral resolution must be considered.

PSPs are propagating modes[8,11] which are strongly damped in their propagation direction due to intrinsic dissipation[13,14] and radiative damping[8,15]. A quantitative measure of how far a PSP mode travels is the propagation length L_x, which is defined by the $1/e$ attenuation of the PSP field in the propagation direction, and is directly related to the imaginary part of the complex PSP wave vector, k_{ix}, by $L_x = (2k_{ix})^{-1}$. If radiative damping can be neglected, L_x is predominantly determined by the complex dielectric function of the metal. As a consequence, L_x is sensitively wavelength-dependent: between $\lambda = 450$ and 1,150 nm, L_x varies for silver by a factor of 50, from 4.4 to 200 μm. L_x, however, determines to what extent PSP modes average over lateral heterogeneities[16]. This means that high spatial resolution in SPM is achieved only for lossy PSP modes, for example with silver only in the ultraviolet spectral range. With gold, however, even for $\lambda \geq 520$ nm, where the onset of the interband transition increases the intrinsic damping considerably, $L_x \leq 1$ μm can be achieved[17].

The countercurrent effects of L_x on spatial resolution and contrast are quite obvious, because decreasing L_x means, from the above, an increase of k_{ix}, and thus an increase of the width of the PSP resonance. As demonstrated in Fig. 4, however, this reduces the contrast between different areas.

Finally, the examples presented above were all based on the contrast between silver areas with LB film coatings of different thicknesses. However, any difference in the optical properties of two materials that manifest themselves in different dispersion curves for PSP can be used to construct an image. In particular one might envisage (1) different metals that carry the PSP field; (2) different indices of refraction (both real and imaginary part) of equally thick coatings; or (3) roughness contrast.

We have restricted the examples to PSP excitation by a prism in the Kretschmann configuration although the Otto set-up, as well as a hybrid configuration (B.R. & W.K., in preparation) or even a grating coupling are feasible. Experiments along these lines are currently under way.

We acknowledge financial support by the Deutsche Forschungsgemeinschaft and by the Leonard-Lorenz-Stiftung, München.

Received 5 October 1987; accepted 5 January 1988.

1. Lösche, M. *et al. Thin Solid Films* **117**, 269-280 (1984).
2. Krug, W., Rienitz, J. & Schulz, G. *Beiträge zur Interferenzmikroskopie* (Akademie, Berlin, 1961).
3. Stenberg, M., Sandström, T. & Stiblert, L. *Mat. Sci. Engng.* **42**, 65-69 (1980).
4. Burstein, E., Chen, W. P., Chen, Y. J. & Hartstein, A. *J. Vacuum Sci. Tech.* **11**, 1004-1024 (1974).
5. Kuhn, H., Möbius, D. & Bücher, H. in *Physical Methods of Chemistry* (eds Weissberger, A. & Rossiter, B. W.) pt IIB, Ch. VII (Wiley, New York, 1972).
6. Rothenhäusler, B. & Knoll, W. *Appl. Phys. Lett.* **51**, 783-785 (1987).
7. Kretschmann, E. *Opt. Commun.* **6**, 185-187 (1972).
8. Raether, H. in *Physics of Thin Flms* (eds. Hass, G., Francombe, M. H. & Hoffmann, R. W.) Vol. **9**, 145-261 (Academic, New York, 1977).
9. Gordon, J. G., II & Swalen, J. D. *Opt. Commun.* **22**, 374-376 (1977).
10. Rothenhäusler, B. & Knoll, W. *Opt. Commun.* **63**, 301-304 (1987).
11. Otto, A. *Optik* **38**, 566-577 (1973).
12. Schoenwald, J., Burstein, E. & Elson, J. M. *Solid State Commun.* **12**, 185-189 (1973).
13. Inagaki, T., Kagami, K. & Arakawa, E. T. *Phys. Rev.* **B24**, 3644-3646 (1981).
14. Rothenhäusler, B., Rabe, J., Korpiun, P. & Knoll, W., *Surface Sci.* **137**, 373-383 (1984).
15. Hornauer, D.-L. *Opt. Commun.* **16**, 76-79 (1976).
16. Rothenhäusler, B. & Knoll, W., *Surface Sci.* **131**, 585-594 (1987).
17. Alexander, R. W., Jr *et al. J. chem. Phys.* **59**, 3492-3494 (1973).

Direct imaging of an adsorbed layer by high-resolution electron microscopy

D. A. Jefferson & P. J. F. Harris*

Department of Physical Chemistry, University of Cambridge, Lensfield Road, Cambridge CB2 1EP, UK

The catalytic activity of metal surfaces can be strongly modified, either detrimentally or beneficially, by the presence of pre-adsorbed material. In understanding these changes in activity it is important to elucidate the structure of the adsorbed layer and its relation to the metal surface. Traditionally this has been achieved by low-energy electron diffraction (LEED), but this requires large single-crystal specimens, which bear no resemblance to real catalysts, and the results are often difficult to interpret. We show here that high-resolution electron microscopy (HREM) can be used to obtain direct images of ordered layers of adsorbed sulphur on the surfaces of very small platinum particles in specimens that closely resemble commercial catalysts. Images of this

* Present address: T.I. Research, Hinxton, Saffron Walden, Essex CB10 1RH, UK

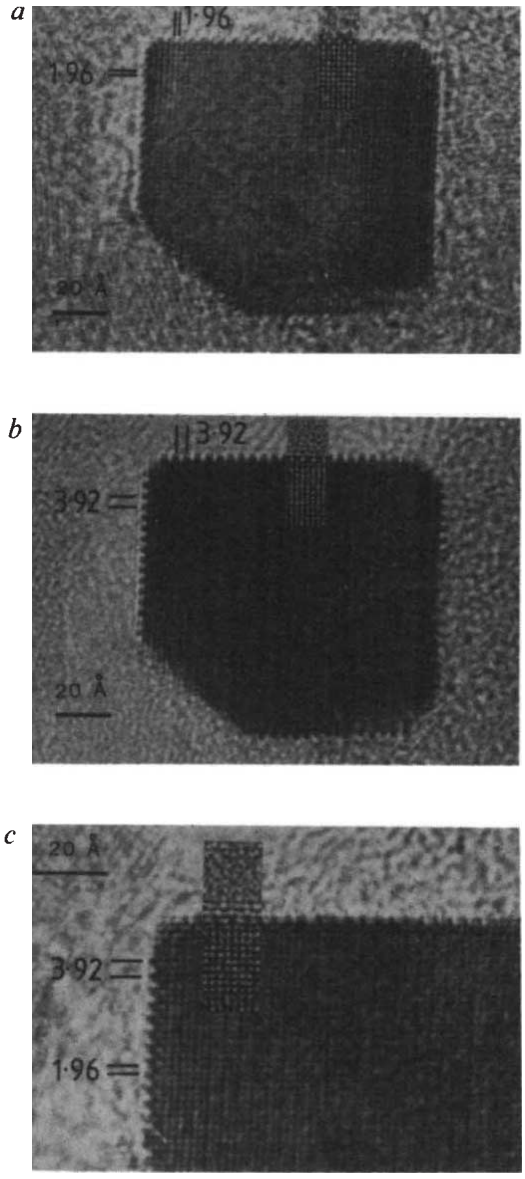

Fig. 1 HREM images of an approximately cubic particle of sulphided platinum, viewed down [100]. *a*, Objective lens defocus of approximately −550 Å; *b*, −250 Å; *c*, −150 Å. Defocus values were determined from the computer-simulated model images discussed in the text, which are shown inset for each. The surface periodicity in *b* and *c* (in ångströms) is indicated.

kind could lead to a more detailed understanding of the interaction of adsorbates with real metal catalysts than has hitherto been possible.

The work described here represents an extension of previous studies which have shown, by conventional bright-field transmission electron microscopy, that heating platinum/alumina specimens in sulphur-containing atmospheres induces (100) faceting of the platinum particles[1,2]. Consequently, single-crystal particles in sulphur-treated specimens often exhibit approximately cubic shapes. This study involved imaging these faceted particles at much higher resolution with a modified JEM-200CX electron microscope developed for the study of ultrafine catalyst particles[3,4], operated at 200 kV. The specimens examined comprised metallic platinum particles of mean size ~113 Å dispersed on a self-supporting alumina film[5,6]. Sulphur deposition was done by heating to 500 °C in a flowing mixture containing 100 p.p.m. of hydrogen sulphide in hydrogen[1,2].

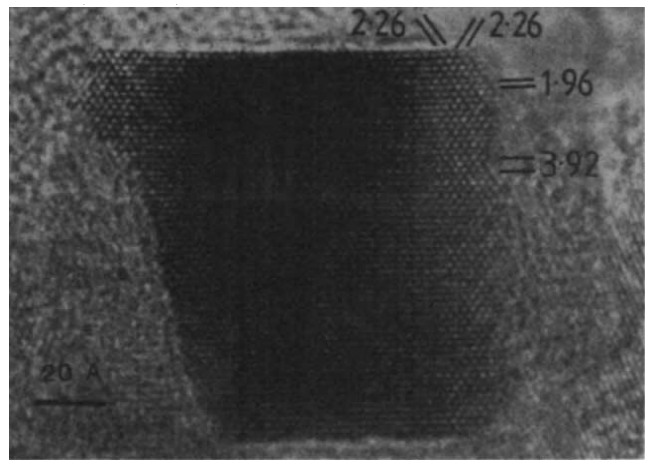

Fig. 2 HREM image of a similar particle to that in Fig. 1, but with one cube edge partly eroded, viewed down [110]. The relevant periodicities (Å) are indicated.

The objective lens characteristics of the microscope used (C_s, 0.52 mm; C_c, 1.05 mm) were such that at a focus slightly beyond the optimum or 'Scherzer' position[7], the interpretable point resolution extended out to 1.95 Å with an absolute information limit of 1.7 Å. As in previous studies of surface restructuring of metals and oxides[8–10], surface detail was observed in profile at the vertical edges of the crystallites, but in this case evidence of an apparent surface superlattice on the upper and lower faces was also noted. Micrographs were recorded at electron-optical magnifications of ~475,000 and 700,000, astigmatism being corrected by observing the granularity of amorphous regions of the specimen support, and particular care was taken to avoid inclination of the incident beam with its attendant difficulties in image interpretation[11]. Observation of the images at greatly enhanced magnification by a television pick-up system was used to ensure that there were no changes in image detail arising from electron irradiation, and no observable carbon contamination was noted.

Typical micrographs of an approximately cubic crystallite of platinum (dimensions perpendicular to the incident beam of 104 Å × 92 Å) are shown in Fig. 1. Figure 1*a* shows an image of the crystal at approximately the optimum focus, with the bulk region showing only the crossed (200) fringes of 1.96 Å spacing, as expected for the [100] orientation of platinum metal, but the bright fringe at the edges of the crystal is clearly of complicated structure, with some indications of a doubling of the repeat distance in the direction parallel to the edge. At a position closer to the gaussian focus (Fig. 1*b*) this doubled repeat (3.92 Å) is clearly evident: furthermore, an apparent doubling of the lattice repeat within the crystal can now be observed. Both features are also evident in the enlarged image of Fig. 1*c*: in this case the focus position is slightly beyond the optimum one and the image contrast is reversed, with the platinum atoms appearing as white dots.

In addition to the [100] projection, images could also be recorded from particles in other directions, a [110] image being shown in Fig. 2. In this case the principal contrast within the crystal comes from two sets of 1.96 Å (200) fringes: the latter are parallel to the straight edges of the crystal. The crystal thickness clearly increases towards a line running down the centre: given the general near-cubic morphology it seems highly probable that Fig. 2 shows a micrograph of a roughly cubic crystal with the electron beam perpendicular to one of the cube edges. In the image of Fig. 2, the bright fringe on the upper and lower (100) faces appears to be perfectly normal, with no increased periodicity, but an apparent doubling of the (200)

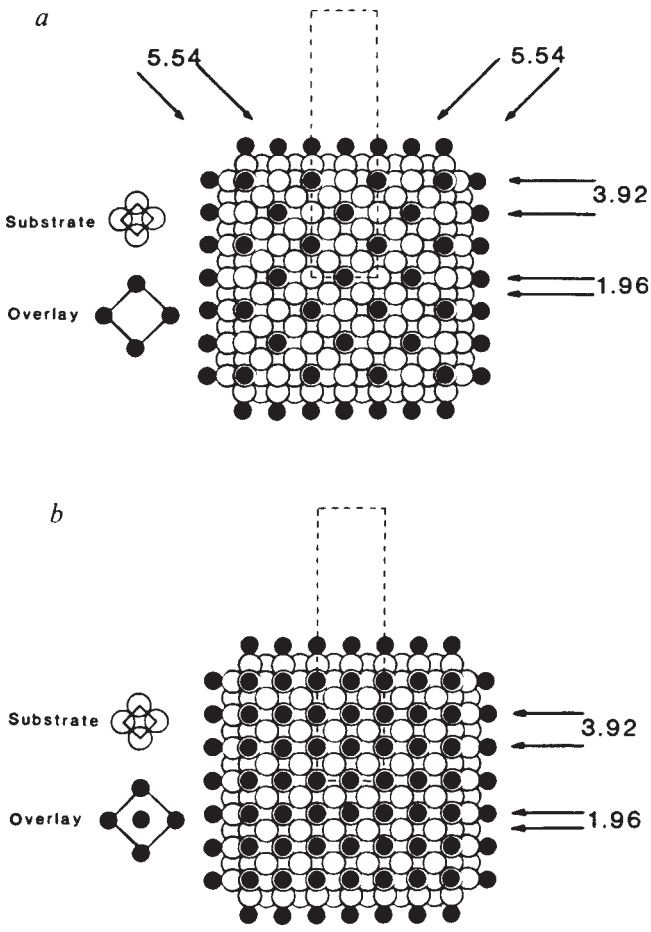

Fig. 3 Diagrammatic arrangements of the two possible sulphur overlays on a small cubic crystal of platninum, viewed down [100]. *a*, p(2×2) overlay; *b*, c(2×2). In both cases the unit cell used for computer image-simulation and the relevant periodicities are indicated.

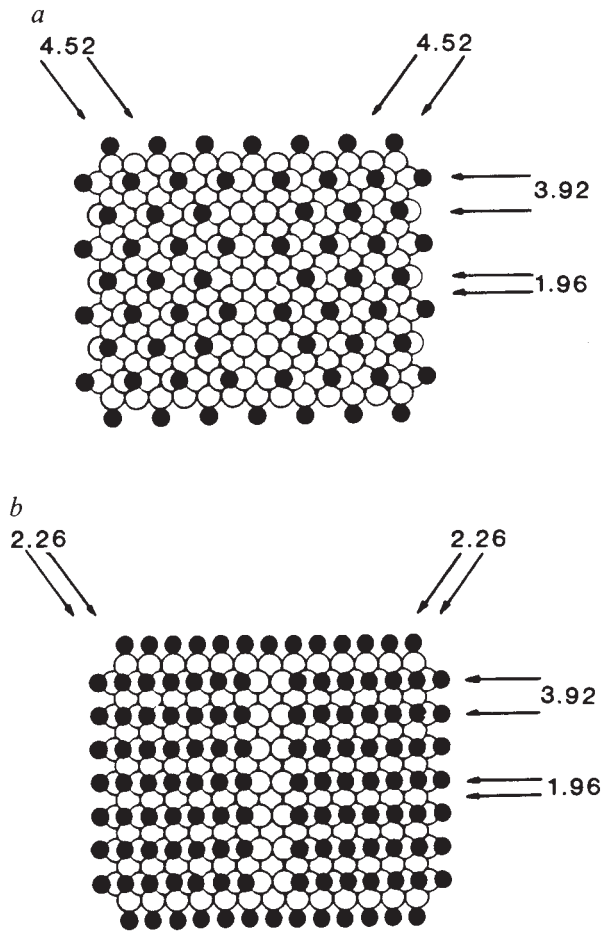

Fig. 4 As for Fig. 3, but with the crystals viewed down the [110] direction.

fringes is observed within the crystal bulk, particularly in the thicker regions.

The surface features observed in these images can arise in three ways; by formation of a surface sulphide, by restructuring of the platinum (100) surface or by the formation of an adsorbed layer of sulphur atoms. As regards the first, the conditions of preparation used were not favourable for the formation of bulk sulphide[12,13]: furthermore, the changes in lattice periodicity expected for an epitaxial sulphide growth were not observed, even though recent work on the growth of Cu_2O on copper[14] has indicated that even a single *complete* layer of oxide can be observed. For the second alternative, there is no LEED evidence to suggest that any restructuring of the platinum (100) face occurs on exposure to sulphur. In addition, restructuring of these faces to produce a doubling of the repeat length at the surface would imply a 'corrugated' (100) surface composed of tiny (110) facets, and although trial image simulations suggest that this could give contrast effects similar to those observed (indeed a surface arrangement of any atom could, at suitable thicknesses, give this contrast), it would seem very unlikely, as the proven effect of sulphur exposure is to eliminate all faces other than (100). Finally, energy-dispersive X-ray emission analysis upon groups of particles definitely indicates the presence of sulphur: consequently we must therefore consider the third alternative, namely that we are observing directly a layer of sulphur adatoms.

To construct a model of adsorbed sulphur which accounts for the observed image contrast, two main factors must be taken into account. Firstly, any arrangement must be compatible with existing LEED studies on macroscopic crystals[15,16], which indicate two possible types of overlays, either primitive or centred 2×2 arrays, corresponding to coverages of 25 and 50%, respectively. The arrangements of sulphur atoms are shown diagrammatically in Figs 3 and 4. When viewed in [100] projection (Fig. 3) it can be seen that both models will produce a doubling of the local repeat on the side faces of the cube, although the p(2×2) case might be expected to give a superlattice of 5.54 Å fringes at 45° to the cube edges on the upper and lower faces of the crystal: this was not observed in practice. In [110] orientation (Fig. 4) the p(2×2) model would give rise to a doubled repeat on the vertical faces, not seen in the real images, whereas the centred overlay would be quite compatible with the experimental observations. Argument on purely geometric grounds, therefore, would favour the c(2×2) adsorbate structure.

Although the geometrical considerations discussed above imply that the image contrast arises from the c(2×2) adsorbate layer, the question of whether or not adsorbed sulphurs can produce sufficient contrast to be observed, especially when viewed against a background of supporting Al_2O_3, remains to be answered. To investigate this, a full set of multislice image simulations[17,18] were done with the quasi-periodic cell indicated

in Fig. 3, with dimensions of 7.82 Å × 31.32 Å, and a sampling interval of 0.06 Å, corresponding to an array size of 512 × 128 potential points. Owing to the extremely strong scattering of the platinum atoms, the slice thickness was 0.654 Å such that each platinum atom was essentially regarded as three scattering centres in a direction parallel to the incident electron beam, and there were three different types of slice, one of which contained only sulphur atoms.

The computations were performed to a crystal thickness of 100 Å, against a 40 Å thick background of amorphous Al_2O_3. Simulation of the contrast from the latter was accomplished by the method of Gai *et al.*[19], taking random coordinates for aluminium and oxygen atoms within each slice computed. For this background, the slice thickness used was 2.5 Å. At one particular defect of focus, all the relevant factors affecting image contrast, namely spherical aberration ($C_s = 0.52$ mm) focus spread (83 Å) and beam divergence (10^{-3} mrad) were included. Owing to the excessive demands on computational resources required by the programs used[20] for this full calculation, however, subsequent simulations were performed without including the last two factors, where it was confirmed that their effect was merely to diminish the overall magnitude of the contrast observed. In such cases the resolution was artificially limited to 1.8 Å.

The results of these simulations are shown as insets on Fig. 1. They confirm that an adsorbed sulphur overlay can indeed produce enough contrast to be visible in the experimental image, and tests with varying thicknesses of amorphous background suggest that this would be valid for the c(2 × 2) overlay until the background medium was at least 120 Å thick. For the p(2 × 2) overlay, where the density of sulphur atoms in projection was only 50% of that for c(2 × 2), the overlay was almost invisible when the background thickness reached 50 Å: consequently we must conclude that the observed images correspond to the latter structure.

Although the results described here refer to an ordered overlay, the use of the HREM technique would allow true imaging of a non-periodic arrangement, if this were present. Exactly how much structural information is obtainable remains to be seen, but in principle, by using multislice procedures, it may be possible to determine the exact location of adsorbate atoms and their spatial relation to those of the support, as the computation involved, although considerable, is less than that required for complete elucidation of a LEED pattern. In such cases we would then have an exceptionally powerful technique for determining the structure of adsorbates on real catalysts.

We thank the SERC for providing electron-microscopic facilities, and the Harwell Laboratory for the provision of materials. D.A.J. is indebted to Dr J. C. Barry, Arizona State University for assistance in the multislice computations. Part of this work was done under a NSF program.

Received 7 December 1987; accepted 16 February 1988.

1. Harris, P. J. F. *Nature* **323,** 792–794 (1986).
2. Harris, P. J. F. *Surface Sci.* **185,** L459–L466 (1987).
3. Jefferson, D. A. *et al. Nature* **323,** 428–431 (1986).
4. Duff, D. G., Curtiss, A. C., Edwards, P. P., Jefferson, D. A. & Johnson, B. F. G. *Angew. Chem.* **26,** 676–678 (1988).
5. Harris, P. J. F., Boyes, E. D. & Cairns, J. A. *J. Catal.* **82,** 127–146 (1983).
6. Harris, P. J. F. *J. Catal.* **97,** 527–542 (1986).
7. Erickson, H. P. & Klug, A. *Phil. Trans. R. Soc.* B **261,** 105–118 (1971).
8. Marks, L. D. & Smith, D. J. *Nature* **303,** 316–318 (1983).
9. Warble, C. E. *Ultramicroscopy* **15,** 301–309 (1984).
10. Smith, D. J., Bursill, L. A. & Jefferson, D. A. *Surface Sci.* **175,** 673–683 (1986).
11. Smith, D. J., Saxton, W. O., O'Keefe, M. A., Wood, G. J. & Stobbs, W. M. *Ultramicroscopy* **11,** 263–282 (1983).
12. Oudar, J. *Catal. Rev. Sci. Eng.* **22,** 171–195 (1980).
13. Bartholomew, C. H., Agrawal, P. K. & Katzer, J. R. *Adv. Catal.* **31,** 135–242 (1982).
14. Curtiss, A. C. *et al. J. phys. Chem.* (in the press).
15. Heegemann, W., Meister, K. H., Bechtold, E. & Hayek, K. *Surface Sci.* **49,** 161–180 (1975).
16. Fischer, T. E. & Kelemen, S. R. *Surface Sci.* **69,** 1–22 (1977).
17. Cowley, J. M. & Moodie, A. F. *Acta crystallogr.* **A10,** 609–619 (1957).
18. Goodman, P. & Moodie, A. F. *Acta crystallogr.* **A30,** 280–290 (1974).
19. Gai, P. L., Goringe, M. J. & Barry, J. C. *J. Microsc.* **142,** 9–24 (1986).
20. Ishizuka, K. thesis, Arizona State Univ. (1986).

Electron microscopy on the $T_C = 110$ K (midpoint) phase in the system Bi_2O_3–SrO–CaO–CuO

H. W. Zandbergen*, Y. K. Huang†, M. J. V. Menken†, J. N. Li, K. Kadowaki†, A. A. Menovsky†, G. van Tendeloo‡ & S. Amelinckx‡

*Gorlaeus Laboratories, State University Leiden, PO Box 9502, 2300 RA Leiden, The Netherlands
†Natuurkundig Laboratorium der Universiteit van Amsterdam, Valckenierstraat 65, 1018 XB Amsterdam, The Netherlands
‡Center for Electron Microscopy, University of Antwerp, RUCA, Groenenborgerlaan 171, Antwerp, Belgium

The system is known to have at least two phases exhibiting high superconducting transition temperatures (T_C) of 85 and 110 K. It is well established that $Bi_2Sr_2CaCu_2O_{8+\delta}$ has a T_C of ~85 K. To date it is not known which phase in the system exhibits $T_C = 110$ K. We performed high-resolution electron microscopy and analytical electron microscopy on material having a nominal composition $BiSrCaCu_2O_x$, and containing a relatively high fraction of the phase with $T_C = 110$ K. Two structures related to the structure of $Bi_2Sr_2CaCu_2O_{8+\delta}$ are found. These structures and their possible compositions are discussed.

Since the discovery of ceramic materials exhibiting high superconducting transition temperatures, much research on these materials has been carried out. One of the goals of the research was to discover materials with a T_C higher than that of the widely studied compound $YBa_2Cu_3O_7$. Because the high T_C is believed to be associated with the two-dimensional nature of $YBa_2Cu_3O_7$, one of the aims of the research was to try to substitute copper in known layered compounds.

One of the layered compounds resembling the perovskite-like structure of $YBa_2Cu_3O_7$ is $Bi_4Ti_3O_{12}$[1]. The structure of this compound is composed of a perovskite block of three units stacked with a Bi_2O_2 layer. A large variety of phases exists, all having that Bi_2O_2 layer, but with a different number of units in the perovskite block. Michel *et al.*[2] studied the superconducting behaviour of a compound, which they reported to be $Bi_2Sr_2Cu_2O_{7+\delta}$ with a T_C of 20 K.

Maeda *et al.*[3] investigated the system CaO–SrO–Bi_2O_3–CuO and found a new superconductor with $T_C = 110$ K, and claimed the composition to be $BiSrCaCu_2O_x$.

Research at many laboratories was immediately focused on this new phase. Many researchers were readily able to synthesize a compound with $T_C \sim 85$ K, but were unable to reproduce the result of Maeda *et al.* The elucidation of the composition and the structure of the 85-K phase took several weeks, suggesting that this material is much more complex than $YBa_2Cu_3O_7$. The structure is found to be very complicated with a long period modulation. The basic structure, however, has been determined by several groups[4], with an approximate composition of $Bi_2Sr_2CaCu_2O_{8+\delta}$.

One of the problems in determining the composition of the compound with T_C of 85 K is the composition range of the material. This is due partly to the existence of a region of solid solution (H. W. Z. *et al.*, manuscript in preparation) with a varying Ca:Sr ratio, but also because defects are introduced[5] in the structure, changing the composition.

Apart from the modulation, a consensus has been obtained on the substructure and its superconducting behaviour. The 110-K material is still unresolved.Here ll reports, this phase was only a minority phase, making it particularly difficult to elucidate its structure and composition.

Here we report an electron microscopy study on a nominal mixture of $BiSrCaCu_2O_X$ exhibiting almost zero resistance and a considerable drop in the magnetization at 107 K. We show